

ZEROI2V: ZERO-COST ADAPTATION OF PRE-TRAINED TRANSFORMERS FROM IMAGE TO VIDEO

Xinhao Li Limin Wang *

State Key Laboratory for Novel Software Technology, Nanjing University, China
xinhaoli00@outlook.com lmwang@nju.edu.cn

ABSTRACT

Adapting image models to video domain is becoming an efficient paradigm for solving video recognition tasks. Due to the huge number of parameters and effective transferability of image models, performing full fine-tuning is less efficient and even unnecessary. Thus, recent research is shifting its focus towards parameter-efficient image-to-video adaptation. However, these adaptation strategies inevitably introduce extra computational cost to deal with the domain gap and temporal modeling in videos. In this paper, our goal is to present a zero-cost adaptation paradigm (ZeroI2V) to transfer the image transformers to video recognition tasks (i.e., introduce zero extra cost to the adapted models during inference). To achieve this goal, we present two core designs. First, to capture the dynamics in videos and reduce the difficulty of achieving image-to-video adaptation, we exploit the flexibility of self-attention and introduce the spatial-temporal dual-headed attention (STDHA) that efficiently endow the image transformers with temporal modeling capability at zero extra parameters and computation. Second, to handle the domain gap between images and videos, we propose a linear adaption strategy which utilizes lightweight densely placed linear adapters to fully transfer the frozen image models to video recognition. Due to its customized linear design, all newly added adapters could be easily merged with the original modules through structural reparameterization after training, thus achieving zero extra cost during inference. Extensive experiments on four widely-used video recognition benchmarks show that our ZeroI2V can match or even outperform previous state-of-the-art methods while enjoying superior parameter and inference efficiency.

1 INTRODUCTION

Adapting pre-trained foundation models such as BERT (Devlin et al., 2019) and GPT (Radford et al., 2018; 2019; Brown et al., 2020) through efficient strategies has yielded excellent performance on downstream tasks in natural language understanding. This new paradigm is becoming popular in computer vision due to the available pre-trained image models such as CLIP (Radford et al., 2021), DINO (Caron et al., 2021; Oquab et al., 2023). These models could be easily adapted to downstream tasks through linear probe, fine-tuning or even zero-shot recognition, exhibiting robustness and strong transfer capabilities similar to those of large-scale language models. Recently, the *parameter-efficient transfer learning* (PETL) (Jia et al., 2022; Chen et al., 2022; Nie et al., 2022; Lin et al., 2022b; Pan et al., 2022) is becoming an efficient paradigm to adapt these large pre-trained models due to their huge numbers of parameters and high computational cost of full fine-tuning.

For video understanding, there exist several large pre-trained video models (Tong et al., 2022; Wang et al., 2023) from self-supervised learning, but these models are of high computational complexity due to the joint spatiotemporal attentions. Therefore, adapting pre-trained image models to video domain through efficient strategies is still a practical solution to video recognition. In fact, the state-of-the-art video networks have long relied on the pre-trained image models by inflating the kernels (Carreira & Zisserman, 2017; Liu et al., 2022a; Arnab et al., 2021; Liu et al., 2022c) or inserting plug-and-play temporal modules (Wang et al., 2016; Lin et al., 2022a; Li et al., 2020; Liu et al., 2021b; Wang et al., 2021a). However, most of these methods necessitate full fine-tuning, which involves updating all the model parameters during training on video datasets. As the scale of pre-trained models increases,

*Corresponding author.

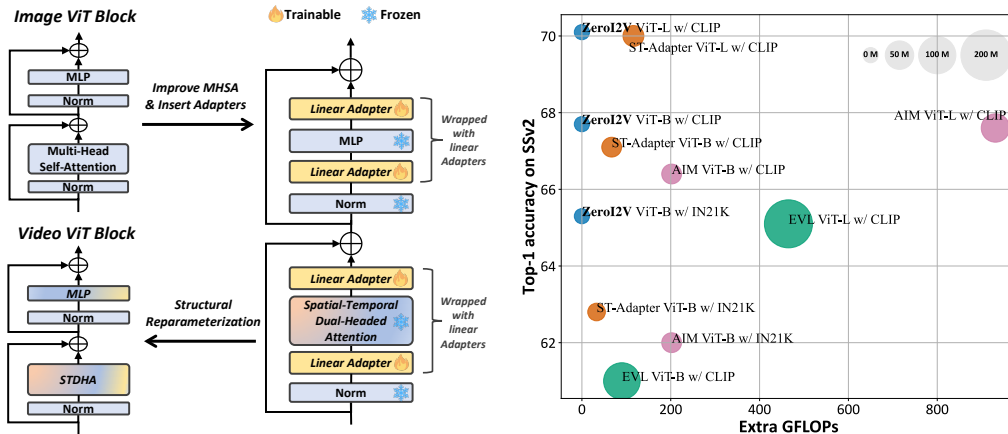


Figure 1: **Left:** Our zero-cost image-to-video transfer learning method. **Right:** Comparison of PETL methods on SSv2 validation set. For more intuitive comparison, the views of the methods in the figure are all $8 \times 3 \times 1$. Two core techniques enable us to achieve superior performance on video tasks without introducing additional computation and parameters during inference.

full fine-tuning becomes impractical due to the high training costs and the risk of overfitting or even catastrophic forgetting when the downstream data is limited. In addition, these methods often inevitably introduce extra cost to the adapted video models due to these newly added modules.

In this paper, we aim to present a new efficient paradigm of adapting image transformers to video downstream tasks with two main objectives. First, inspired by the PETL methods in NLP (Houlsby et al., 2019; Lester et al., 2021; Hu et al., 2022; Li & Liang, 2021) and Images (Jia et al., 2022; Chen et al., 2022; Nie et al., 2022), we aim to devise a parameter-efficient transfer technique from image to video, which can effectively reduce the risk of over-fitting and greatly improve the training efficiency. Second, to overcome the issue of high computation in the adapted video models, we try to present a zero-cost adaptation method without introducing any extra computations to the final video models during inference. This zero-cost adaptation would allow for more efficient deployment of transferred video models in the real applications.

To achieve the above two objectives, we propose a novel zero-cost transfer learning method (as shown in Figure 1) that can utilize the off-the-shelf pre-trained image transformers to *achieve excellent performance on video tasks without additional parameters and computation during inference*. To be specific, for the temporal modeling required for video tasks, we transform multi-head self-attention into *spatio-temporal dual-head attention* (STDHA) by reassigning some heads to achieve temporal modeling at zero computation and zero parameters. For image-to-video transfer, we explore the strategy of using linear adapters to fully adapt the parameters of each part of the model and merge them with the frozen original parameters through structural reparameterization after training, thus achieving zero-cost during inference.

To summarize, we make the following contributions: **1)** We propose a new approach for *parameter-efficient image-to-video transfer learning* that can achieve the zero-cost adaptation of transformers from image to video without introducing additional computation and parameters during inference. **2)** We introduce a novel attention mechanism named *Spatio-Temporal Dual-Headed Attention* (STDHA), which utilizes the flexibility of self-attention to achieve temporal modeling without introducing extra computation and parameters. **3)** To the best of our knowledge, we are the first to investigate the achievement of zero-cost image-to-video adaptation through the utilization of a linear structure. And we establish a benchmark in this field by conducting extensive experiments with a diverse range of adaptation strategies. **4)** Our method achieves comparable or even better performance than state-of-the-art methods on four action recognition benchmarks while enjoying the advantage of parameter and inference efficiency.

2 RELATED WORK

Pre-trained image transformers The powerful scalability of ViT (Dosovitskiy et al., 2021) brings more possibilities to the pre-trained image model. In addition to the traditional supervised ap-

proach (Dosovitskiy et al., 2021; Zhai et al., 2022; Liu et al., 2022b), recent works (He et al., 2020; Bao et al., 2022; Caron et al., 2021; He et al., 2022a; Oquab et al., 2023) utilize self-supervised learning to effectively learn representations from unlabeled data. Moreover, several works (Radford et al., 2021; Li et al., 2022a; Tschannen et al., 2022; Cherti et al., 2022) adopt large-scale multi-modal data (*e.g.*, text-image pairs) to learn visual representations with great transferability. Our proposed adaptation strategy can leverage these off-the-shelf pre-trained image transformers to achieve outstanding performance on video tasks.

Video action recognition State-of-the-art methods for video action recognition have long relied on image models. Previous works for action recognition can be classified into two categories: one is to extend the image model for spatial-temporal modeling by inflating weights and structures (Carreira & Zisserman, 2017; Feichtenhofer et al., 2019; Feichtenhofer, 2020; Liu et al., 2022c; Li et al., 2022b; Fan et al., 2021; Li et al., 2022c), while the other is to directly utilize the image model as the backbone and insert plug-and-play modules for temporal modeling (Wang et al., 2016; Zhou et al., 2018; Lin et al., 2022a; Liu et al., 2021b; Wang et al., 2021a). Following the success of new training paradigms in image, several works have attempted to learn transferable video representations via self-supervised learning (Tong et al., 2022; Wang et al., 2022; Lu et al., 2023; Wang et al., 2023) or multi-modal video-text pre-training (Li & Wang, 2020; Wang et al., 2021b; Ni et al., 2022). However, the above methods usually require full fine-tuning of the entire model or training from scratch, resulting in high training costs and additional computational overhead. In this work, we avoid the above problems by adapting the pre-trained image transformers to video tasks in an efficient manner.

Parameter-efficient transfer learning To address the issue of training inefficiency caused by the continuous growth of model size, Parameter-efficient transfer learning (PETL) is initially introduced in NLP (Houlsby et al., 2019; Pfeiffer et al., 2020; 2021; Lester et al., 2021; Li & Liang, 2021; Hu et al., 2022; Zaken et al., 2022) and subsequently applied to vision tasks (Jia et al., 2022; Lian et al., 2022; He et al., 2022b; Chen et al., 2022; Nie et al., 2022). These techniques aim to achieve comparable or even superior performance on other tasks by fine-tuning only a small subset of trainable parameters. Most PETL methods (Jia et al., 2022; Chen et al., 2022; He et al., 2022b; Lian et al., 2022; Zhang et al., 2022; Nie et al., 2022) in vision domain are limited to transfer within the same modality (*e.g.*, image-to-image or video-to-video). In contrast, our research focuses on image-to-video transfer learning. Despite progress made by recent studies (Lin et al., 2022b; Pan et al., 2022; Yang et al., 2023), these methods require additional computation and parameters for temporal modeling of video tasks and image-to-video adaptation. For example, EVL (Lin et al., 2022b) incorporates an additional temporal transformer decoder, while ST-Adapter (Pan et al., 2022) introduces additional adapters with depth-wise 3D convolution layers. Similarly, AIM (Yang et al., 2023) adds extra adapters and necessitates an additional time attention calculation at each block. In contrast to previous works, our proposed method eschews the introduction of additional computation or parameters during inference, yet still achieves comparable or superior performance compared to previous methods.

3 METHODOLOGY

In this section, we first briefly revisit the basic block of ViT (Sec. 3.1), and then discuss how to utilize the flexibility of self-attention to achieve temporal modeling without introducing additional computation and parameters (Sec. 3.2). Finally, we explain how we implement zero-cost image-to-video adaptation with a serial linear structure (Sec. 3.3).

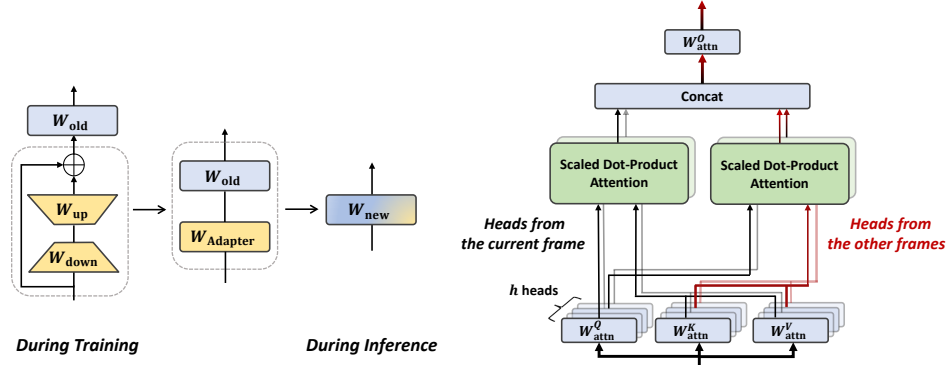
3.1 PRELIMINARY

The original ViT (Dosovitskiy et al., 2021) block consists of two types of network layers: multi-head self-attention (MHSA) and multi-layer perceptron (MLP). As shown in Figure 1, a ViT block consists of MHSA and MLP connected in series in a residual structure:

$$z_l = x_l + \text{MHSA}(\text{LN}(x_l)), \quad (1)$$

$$x_{l+1} = z_l + \text{MLP}(\text{LN}(z_l)), \quad (2)$$

where LN denotes layer normalization (Ba et al., 2016) and x_l represents the input to the l -th ViT block. Then we review their specific implementation details, for the sake of simplicity, we ignore the bias and denote $X \in \mathbb{R}^{n \times d}$ as input of MHSA and MLP.



(a) Layer merging via structural reparameterization (b) Spatial-temporal dual-headed attention

Figure 2: **Illustration of the proposed linear adaptation and STDHA.**

MHSA first performs three different linear projections $W_{\text{attn}}^Q, W_{\text{attn}}^K, W_{\text{attn}}^V \in \mathbb{R}^{d \times d}$ on the input X to obtain the query Q and key-value pairs K, V . These are then evenly divided into h heads by channel. Each head independently performs the scaled dot-product attention calculation. Finally, the heads are concatenated by channel and then a linear projection $W_{\text{attn}}^O \in \mathbb{R}^{d \times d}$ is performed to obtain the final calculation result:

$$Q, K, V = XW_{\text{attn}}^Q, XW_{\text{attn}}^K, XW_{\text{attn}}^V, \quad (3)$$

$$\text{head}_i = \text{Attention}(Q_i, K_i, V_i), \quad (4)$$

$$\text{MHSA}(X) = \text{Concat}(\text{head}_1, \dots, \text{head}_h)W_{\text{attn}}^O. \quad (5)$$

MLP involves two linear projections $W_{\text{mlp}}^{\text{up}} \in \mathbb{R}^{d \times d'}$, $W_{\text{mlp}}^{\text{down}} \in \mathbb{R}^{d' \times d}$, $d' > d$ and one non-linear activation function σ :

$$\text{MLP}(X) = \sigma(XW_{\text{mlp}}^{\text{up}})W_{\text{mlp}}^{\text{down}}. \quad (6)$$

3.2 ZERO-COST TEMPORAL MODELING

Applying image models to video tasks often requires the incorporation of additional modules for temporal modeling, which not only introduces additional parameters and computation, but also results in additional training costs. In this work, we address temporal modeling from three key perspectives: (1) Offering powerful capabilities for temporal modeling. (2) Reducing the difficulty of image-to-video adaptation. (3) Minimizing the introduction of additional computation and parameters compared to the original model.

Michel et al. (2019) suggests that most heads are redundant given the rest of the model. Inspired by this, we attempt to reassign some heads as *temporal heads* in the multi-head attention to perform temporal modeling tasks, while the remaining heads continue to perform their original spatial modeling tasks as *spatial heads*, thereby achieving efficient spatial-temporal modeling.

Spatial-temporal dual-headed attention (STDHA) As depicted in Figure 2b, given an input sequence $X = \{x_1, x_2, \dots, x_T\}$ in which $x_t \in \mathbb{R}^{n \times d}$, assuming that the query and key-value pairs obtained after linear projection of the x_t are $Q^t, K^t, V^t \in \mathbb{R}^{n \times d}$. We divide the h heads of the MHSA into two groups of size $n - k$ and k . One group of heads queries the key-value pairs at the current time t to perform *spatial modeling*, while the other group of heads queries the key-value pairs at other times $t + \Delta t_i$ to perform *temporal modeling*. Finally, the information from the two groups of heads is aggregated by a linear projection to perform *spatial-temporal modeling*:

$$\text{S-head}_i = \text{Attention}(Q_i^t, K_i^t, V_i^t), \quad (7)$$

$$\text{T-head}_i = \text{Attention}(Q_i^t, K_i^{t+\Delta t_i}, V_i^{t+\Delta t_i}) (\Delta t_i \neq 0), \quad (8)$$

$$\text{STDHA}(X) = \text{Concat}(\text{T-head}_1, \dots, \text{T-head}_k, \text{S-head}_{k+1} \dots \text{S-head}_h)W_{\text{attn}}^O, \quad (9)$$

where Δt_i represents the time offset of the key-value pair of the i -th head. We did not directly use temporal attention or temporal convolution for the temporal modeling like previous works (Lin

et al., 2022b; Pan et al., 2022; Yang et al., 2023). Instead, we design a more efficient spatiotemporal modeling operator by decoupling spatial modeling and temporal modeling to different heads:

- For the spatial head, it still only needs to complete the spatial modeling task as the original image transformer, which reduces the difficulty of achieving image-to-video adaptation.
- For the temporal head, it actually implements the inter-frame attention mechanism with frames at different times. Zhang et al. (2023) have demonstrated the effectiveness of inter-frame attention mechanism for modeling motion information, which is crucial for action recognition tasks. In addition, as shown in Table 1c, we can achieve both short-distance and long-distance modeling by controlling the Δt_i of the temporal head, which enables us to achieve enhanced temporal modeling capabilities.

Comparison with other zero-cost operators There have been several previous attempts (Bulat et al., 2021; Zhang et al., 2021; Xiang et al., 2022) to use image transformers to achieve efficient temporal modeling at zero parameters and zero computation. For example, Bulat et al. (2021) achieves approximations to full space-time attention by mixing tokens from adjacent frames. Zhang et al. (2021) performs temporal modeling by using channel shift on the cls tokens of different frames. Xiang et al. (2022) mixes information from adjacent frames using temporal patch shift and temporal channel shift before MHSA. However, these methods do not take advantage of the inherent characteristics of the transformer structure. By decoupling the learning of spatial and temporal information with head relocation, STDHA maintains the *purity of key-value pair information* within the same head, thereby achieving better spatial-temporal information learning than other zero-cost temporal modules. And STDHA *simultaneously captures both short-range and long-range dependencies*, rather than being limited to adjacent frames. As shown in the Table 1, these two key distinctions enable our STDHA to achieve superior spatial-temporal modeling.

3.3 ZERO-COST IMAGE-TO-VIDEO ADAPTATION

Inspired by LoRA (Hu et al., 2022), we can fine-tune the model using a linear structure and then merge it with the original model during inference. However, to deal with the domain gap between images and videos, previous works (Lin et al., 2022b; Yang et al., 2023; Pan et al., 2022) often use nonlinear structures to achieve stronger transfer capabilities. Therefore, we need to further consider how to achieve effective image-to-video transfer using only a linear structure.

Layer merging via structural reparameterization Assuming that the frozen weights of the original model are W_{old} and the new trainable weights are W_{new} . Reviewing the structure of LoRA, it uses a low-rank decomposition matrix W_{LoRA} parallel to the original weights:

$$W_{\text{new}} = W_{\text{LoRA}} + W_{\text{old}} = W_{\text{up}}W_{\text{down}} + W_{\text{old}}. \quad (10)$$

In this work, we use a serial linear structure called *Linear Adapter* to fine-tune the original parameters. As shown in Figure 2a, we use structural reparameterization to perform layer merging after training:

$$W_{\text{new}} = W_{\text{Adapter}}W_{\text{old}} = (I + W_{\text{up}}W_{\text{down}})W_{\text{old}}, \quad (11)$$

where I is the identity matrix, $W_{\text{up}} \in \mathbb{R}^{m \times k}$, $W_{\text{down}} \in \mathbb{R}^{k \times n}$, bottleneck width $k \ll \min(m, n)$. As seen in Table 2, compared to parallel structures, serial structures can be more flexibly inserted into the network structure (e.g., for non-square matrices, under the same bottleneck dimension, using LoRA requires a larger number of parameters compared to Linear Adapter), which endows it with better transfer capabilities.

Full adaptation with densely placed linear adapters By observing the structure of MHSA and MLP, we can see that all their trainable parameters concentrate on the linear projections at both ends of the structure. Therefore, fine-tuning the model essentially updates these linear projections. Previous works (Yang et al., 2023; Pan et al., 2022) often selectively tune part of the parameters (e.g., placing only an adapter before MHSA) instead of tuning all parameters to avoid excessive additional computational and parameter costs, while we can achieve zero-cost *full adaptation* by tuning all parameters through wrapping MHSA and MLP with linear adapters. Table 2 shows that full adaptation enables us to achieve excellent image-to-video transfer performance with a linear structure, compensating for the performance degradation caused by the removal of nonlinearity.

Table 1: **Ablation study on STDHA.** Most of the symbols in the table have been declared in the methodology section3. (a) R_c denotes channel change ratio, "Shift" refers to temporal channel shift, while "HR" denotes head relocation as used by STDHA. (b) We use a multiset to represent the time offsets of different heads (*e.g.*, "1 · 2" means that there are 2 heads with $\Delta t = 1$). When $\Delta t=0$, it represents a spatial head. (c) "Temporal RF" refers to temporal receptive field of a single STDHA.

| (a) Comparison of temporal modeling methods, | | | (b) Effect of the number of temporal heads | | | |
|--|-------------------|-------------|--|---|-----|-------------|
| R_c | Method | Top-1 | Backbone | Δt of heads | k | Top-1 |
| 1/6 | [cls] token shift | 61.4 | ViT-B ($h=12$) | $\{1 \cdot \frac{1}{2}, -1 \cdot \frac{1}{2}, 0 \cdot 11\}$ | 1 | 64.8 |
| | Shift QKV | 64.5 | | $\{1 \cdot 1, -1 \cdot 1, 0 \cdot 10\}$ | 2 | 66.0 |
| | Shift KV | 64.6 | | $\{1 \cdot 2, -1 \cdot 2, 0 \cdot 8\}$ | 4 | 65.6 |
| | HR QKV | 64.8 | | $\{1 \cdot 3, -1 \cdot 3, 0 \cdot 6\}$ | 6 | 65.6 |
| | HR KV (STDHA) | 66.0 | | | | |
| 1/4 | Shift KV | 64.0 | ViT-L ($h=16$) | $\{1 \cdot 1, -1 \cdot 1, 0 \cdot 14\}$ | 2 | 67.7 |
| | HR KV (STDHA) | 65.8 | | $\{1 \cdot 2, -1 \cdot 2, 0 \cdot 12\}$ | 4 | 68.5 |
| | | | | $\{1 \cdot 3, -1 \cdot 3, 0 \cdot 10\}$ | 6 | 68.3 |

| (c) Effect of temporal receptive field at at different input lengths. | | | |
|---|---|-------------|-------------|
| Frames | Δt of heads | Temporal RF | Top-1 |
| 8 | $\{1 \cdot 1, 0 \cdot 11\}$ | 2 | 64.7 |
| | $\{1 \cdot 1, -1 \cdot 1, 0 \cdot 10\}$ | 3 | 66.0 |
| | $\{1 \cdot 1, -1 \cdot 1, 2 \cdot 1, 0 \cdot 9\}$ | 4 | 65.5 |
| | $\{1 \cdot 1, -1 \cdot 1, 2 \cdot 1, -2 \cdot 1, 0 \cdot 8\}$ | 5 | 65.7 |
| 16 | $\{1 \cdot 1, -1 \cdot 1, 0 \cdot 10\}$ | 3 | 67.2 |
| | $\{1 \cdot 1, -1 \cdot 1, 2 \cdot 1, 0 \cdot 9\}$ | 4 | 67.3 |
| | $\{1 \cdot 1, -1 \cdot 1, 2 \cdot 1, -2 \cdot 1, 0 \cdot 8\}$ | 5 | 67.8 |
| | $\{1 \cdot 1, -1 \cdot 1, 2 \cdot 1, -2 \cdot 1, 3 \cdot 1, 0 \cdot 7\}$ | 6 | 67.6 |
| | $\{1 \cdot 1, -1 \cdot 1, 2 \cdot 1, -2 \cdot 1, 3 \cdot 1, -3 \cdot 1, 0 \cdot 6\}$ | 7 | 67.3 |
| 32 | $\{1 \cdot 1, -1 \cdot 1, 0 \cdot 10\}$ | 3 | 67.3 |
| | $\{1 \cdot 1, -1 \cdot 1, 2 \cdot 1, 0 \cdot 9\}$ | 4 | 67.8 |
| | $\{1 \cdot 1, -1 \cdot 1, 2 \cdot 1, -2 \cdot 1, 0 \cdot 8\}$ | 5 | 68.5 |
| | $\{1 \cdot 1, -1 \cdot 1, 2 \cdot 1, -2 \cdot 1, 3 \cdot 1, 0 \cdot 7\}$ | 6 | 68.6 |
| | $\{1 \cdot 1, -1 \cdot 1, 2 \cdot 1, -2 \cdot 1, 3 \cdot 1, -3 \cdot 1, 0 \cdot 6\}$ | 7 | 68.4 |
| | $\{1 \cdot 1, -1 \cdot 1, 2 \cdot 1, -2 \cdot 1, 3 \cdot 1, -3 \cdot 1, 4 \cdot 1, 0 \cdot 5\}$ | 8 | 68.2 |

4 EXPERIMENTS

4.1 EXPERIMENTS SETUP

We evaluate our method on four widely-used video recognition benchmarks: two large-scale datasets, namely Kinetics-400 (K400) (Carreira & Zisserman, 2017) and Something-Something V2 (SSv2) (Goyal et al., 2017), in addition to two smaller-scale datasets, UCF101 (Soomro et al., 2012) and HMDB51 (Kuehne et al., 2011). This diverse dataset selection allows for a comprehensive evaluation of our model across various scales and domains. The specific model configuration and training strategy also can be found in the Appendix A. For most main experiments, we use ViT-B and ViT-L pre-trained by CLIP (Radford et al., 2021) as our backbone models, and the additional results using other backbone architectures and pretrained weights can be found in the Appendix B.

4.2 ABLATION STUDY

To validate the effectiveness of our method on image-to-video transfer and temporal modeling, we first conduct ablation experiments on the SSv2 dataset. All ablation experiments were performed using ViT-B/16 with 8 input frames unless specified.

Effectiveness of STDHA Table 1a compares STDHA with other zero-cost temporal modeling methods. The [cls] token shift is implemented according to the original paper (Zhang et al., 2021), with [cls] token shift performed before MHA and MLP. The temporal channel shift operation refers to TPS (Xiang et al., 2022), which shifts a portion of the channels for each head. It can be seen that STDHA significantly outperforms other methods at the same channel change ratio, demonstrating the importance of preserving the purity of information within each head.

Table 2: **Comparison of adaption strategies.** "Width" refers to the bottleneck width of LoRA/Adapter. "Tunable Params" refers to extra trainable parameters besides the parameters of the ViT backbone and linear classifier. "✓" and "✗" indicate whether the corresponding weights have undergone fine-tuning, and "✓" indicates that W_{attn}^Q , W_{attn}^K and W_{attn}^V share the same adapter. "Latency" refers the latency of inference with 3 test samples. All results are obtained using a same V100-32G with PyTorch-builtin mixed precision.

| Method | Weights of ViT block | | | | | | Tunable Params (M) | Bottleneck Width | Latency (ms) | SSv2 Top-1 |
|-------------------------------|----------------------|---------------------|---------------------|---------------------|------------------------------|--------------------------------|--------------------|------------------|--------------|-------------|
| | W_{attn}^Q | W_{attn}^K | W_{attn}^V | W_{attn}^O | $W_{\text{mlp}}^{\text{up}}$ | $W_{\text{mlp}}^{\text{down}}$ | | | | |
| Full Fine-tuning | ✓ | ✓ | ✓ | ✓ | ✓ | ✓ | 86 | - | 28.9 | 63.2 |
| Linear Probe | ✗ | ✗ | ✗ | ✗ | ✗ | ✗ | 0 | - | 28.9 | 20.0 |
| Only tuning temporal head | ✓ | ✓ | ✓ | ✓ | ✗ | ✗ | 4.6 | - | 28.9 | 59.6 |
| ST-Adapter (Pan et al., 2022) | ✓ | ✓ | ✓ | ✓ | ✓ | ✓ | 14 | 192 | 41.0 | 66.2 |
| | ✓ | ✓ | ✓ | ✗ | ✓ | ✗ | 14 | 384 | 38.8 | 65.8 |
| LoRA (Hu et al., 2022) | ✓ | ✗ | ✓ | ✗ | ✗ | ✗ | 7 | 192 | | 64.2 |
| | ✓ | ✓ | ✓ | ✓ | ✗ | ✗ | 14 | 192 | | 65.0 |
| | ✓ | ✗ | ✓ | ✗ | ✓ | ✓ | 25 | 192 | | 64.3 |
| | ✓ | ✗ | ✓ | ✗ | ✓ | ✓ | 17 | 128 | 28.9 | 65.6 |
| | ✓ | ✓ | ✓ | ✓ | ✓ | ✓ | 32 | 192 | | 65.0 |
| | ✓ | ✓ | ✓ | ✓ | ✓ | ✓ | 21 | 128 | | 65.5 |
| Adapter w/ GELU | ✓ | ✓ | ✓ | ✓ | ✓ | ✓ | 7 | 96 | 37.3 | 65.6 |
| | ✓ | ✓ | ✓ | ✗ | ✓ | ✗ | 7 | 192 | 34.9 | 64.6 |
| | ✓ | ✓ | ✓ | ✓ | ✓ | ✗ | 10 | 192 | 36.3 | 66.1 |
| | ✓ | ✓ | ✓ | ✓ | ✓ | ✓ | 14 | 192 | 38.4 | 66.1 |
| Linear Adapter (Ours) | ✓ | ✓ | ✓ | ✓ | ✓ | ✓ | 7 | 96 | | 65.0 |
| | ✓ | ✓ | ✓ | ✗ | ✓ | ✗ | 7 | 192 | | 64.4 |
| | ✓ | ✓ | ✓ | ✓ | ✓ | ✓ | 10 | 192 | | 65.2 |
| | ✓ | ✓ | ✓ | ✓ | ✓ | ✓ | 14 | 192 | 28.9 | 66.0 |
| | ✓ | ✓ | ✓ | ✓ | ✓ | ✓ | 20 | 192 | | 66.3 |
| | ✓ | ✓ | ✓ | ✓ | ✓ | ✓ | 14 | 128 | | 66.2 |

Effect of the number of temporal heads and temporal receptive field We examined the influence of the number of temporal heads and the temporal receptive field in ViT-B and ViT-L. Our findings, detailed in Tables 1b and 1c, suggest that the optimal proportion of temporal heads in ViT lies between 1/6 and 1/4. Regarding the temporal receptive field, our results indicate that for 8-frame inputs, a field of 3 is sufficient, while for longer inputs (16 or 32 frames), performance improves with an increase in the field from 3, saturating at around 5 or 6. Consequently, we employ different STDHA configurations based on input length.

Comparison of adaptation strategies In Table 2, we compare the image-to-video transfer ability of our method with a diverse range of commonly used adaptation methods. For a fair comparison, we all use STDHA with the same setting to provide temporal modeling capabilities. From the results, we can observe that:

- Even with only a small number of parameters being fine-tuned, our linear adapter tuning significantly outperforms full fine-tuning (66.3 vs 63.2). Despite updating the fewest parameters, linear probe performs poorly in image-to-video transfer.
- Even if we only tune the temporal head, we can still achieve about 95% of the full fine-tuning performance. This suggests that extensive fine-tuning of the spatial head may not be necessary to attain satisfactory transfer performance due to *the decoupling of spatial and temporal modeling reduces the difficulty of adaptation*.
- Our *Full Adaptation* strategy is not only effective for linear adapters, but also for non-linear adapters such as the ST-Adapter and GELU Adapter. It not only enhances their adaptation performance, but also *eliminates the performance gap between linear and non-linear structures*. This allows us to achieve zero-cost image-to-video adaptation using linear structures.
- Due to the inflexibility of the parallel structure, for non-square matrices like W_{mlp} , LoRA requires more parameters under the same bottleneck width. It needs to decrease the bottleneck width of the low-rank matrix to align it with the number of parameters of the

Table 3: **Results on Kinetics-400 validation set.** Views = #frames \times #spatial crops \times #temporal clips. “GFLOPs” means 10^9 FLOPs, “M” means 10^6 . “Extra GLOPs” refers to the extra computation added to the original ViT under the same number of views. “New Params” refers to additional parameters during inference besides the parameters of the original ViT backbone and linear classifier.

| Methods | Pretrain | Views | GFLOPs | Extra GFLOPs | Param(M) | New Param(M) | Top-1 | Top-5 |
|--|----------|---------------------------|--------|--------------|----------|--------------|-------------|-------------|
| <i>Methods with full fine-tuning</i> | | | | | | | | |
| UniFormer-B (Li et al., 2022b) | IN1K | 32 \times 3 \times 4 | 3108 | - | 50 | - | 83.0 | 95.4 |
| TimeSformer-L (Bertasius et al., 2021) | IN21K | 96 \times 3 \times 1 | 7140 | - | 121 | - | 80.7 | 94.7 |
| VideoSwin-L (Liu et al., 2022c) | IN21K | 32 \times 3 \times 4 | 7248 | - | 197 | - | 83.1 | 95.9 |
| MViTv2-L(\uparrow 312) (Li et al., 2022c) | IN21K | 40 \times 5 \times 3 | 42420 | - | 218 | - | 86.1 | 97.0 |
| ViViT-L/16x2 FE (Arnab et al., 2021) | JFT | 32 \times 3 \times 1 | 11940 | - | 311 | - | 83.5 | 94.3 |
| MTV-L (Yan et al., 2022) | JFT | 32 \times 3 \times 4 | 18050 | - | 876 | - | 84.3 | 96.3 |
| ViT-B/16 (Pan et al., 2022) | CLIP | 8 \times 1 \times 3 | 422 | 0 | 86 | 0 | 81.0 | 95.5 |
| ActionCLIP-B/16 (Wang et al., 2021b) | CLIP | 32 \times 3 \times 10 | 16893 | 13 | 142 | 56 | 83.8 | 97.1 |
| X-CLIP ViT-L/14 (Ni et al., 2022) | CLIP | 8 \times 3 \times 4 | 7896 | 107 | 420 | 116 | 87.1 | 97.6 |
| Text4Vis ViT-L/14 (Wu et al., 2023) | CLIP | 32 \times 3 \times 4 | 19944 | - | 347 | 43 | 87.1 | 97.4 |
| <i>Methods with PETL</i> | | | | | | | | |
| VideoPrompt ViT-B/16 (Ju et al., 2022) | CLIP | 16 \times 5 \times 1 | - | - | - | - | 76.9 | 93.5 |
| ST-Adapter ViT-B/16 (Pan et al., 2022) | CLIP | 32 \times 1 \times 3 | 1821 | 133 | 93 | 7 | 82.7 | 96.2 |
| EVL ViT-L/14 (Lin et al., 2022b) | CLIP | 8 \times 1 \times 3 | 2022 | 76 | 362 | 58 | 86.3 | - |
| AIM ViT-L/14 (Yang et al., 2023) | CLIP | 32 \times 1 \times 3 | 11208 | 3425 | 341 | 38 | 87.5 | 97.7 |
| ZeroI2V ViT-B/16 | CLIP | 8 \times 1 \times 3 | 422 | 0 | 86 | 0 | 83.0 | 95.8 |
| ZeroI2V ViT-B/16 | CLIP | 16 \times 1 \times 3 | 844 | 0 | 86 | 0 | 83.4 | 96.2 |
| ZeroI2V ViT-B/16 | CLIP | 32 \times 1 \times 3 | 1688 | 0 | 86 | 0 | 83.7 | 96.4 |
| ZeroI2V ViT-L/14 | CLIP | 8 \times 1 \times 3 | 1946 | 0 | 304 | 0 | 86.3 | 97.4 |
| ZeroI2V ViT-L/14 | CLIP | 16 \times 1 \times 3 | 3892 | 0 | 304 | 0 | 86.8 | 97.6 |
| ZeroI2V ViT-L/14 | CLIP | 32 \times 1 \times 3 | 7783 | 0 | 304 | 0 | 87.2 | 97.6 |

linear adapter. However, this reduction in bottleneck width can limit its adaptation ability, ultimately leading to results that are significantly worse than those of the Linear Adapter.

4.3 COMPARISONS WITH THE STATE OF THE ART

Results on K400 As shown in Table 3, our method has significant advantages over traditional full fine-tuning methods, achieving better performance with much lower computational cost. For example, our ZeroI2V ViT-L/14 with an input of 8 frames outperforms MViTv2 (Li et al., 2022c) (86.3 vs 86.1), while requiring more than 20 times fewer GFLOPs (1946 vs 42420). For a ViT-B/16 backbone pre-trained with CLIP, compared to a ViT obtained by full fine-tuning directly, our method achieved a significant performance improvement (83.0 vs. 81.0) with the same number of parameters and GFLOPs, while only updating a small portion of the weights during training (14M vs 86M). Compared to multi-modal methods such as ActionCLIP (Wang et al., 2021b) and X-CLIP (Ni et al., 2022), which require an additional text branch and fine-tune the entire model end-to-end, our ZeroI2V can achieve comparable performance using only the visual encoder. Moreover, although our proposed ZeroI2V doesn’t increase computational or parameter costs during inference compared with the previous PETL method, it can still achieve similar or even better performance. For example, on ViT-B/16, ZeroI2V with an input of 8 frames can surpass ST-Adapter (Pan et al., 2022) with an input of 32 frames (83.0 vs 82.7) with much lower GFLOPs (422 vs 1821). On ViT-L/14, ZeroI2V achieves the same performance as EVL (Lin et al., 2022b), which requires an additional 58M parameters. And ZeroI2V achieves comparable performance to AIM (Yang et al., 2023) (87.2 vs 87.5) with a nearly 30% reduction in GFLOPs (7783 vs 11208).

Results on SSv2 As shown in Table 4, thanks to the effectiveness of STDHA in temporal modeling, our method achieves **72.2%** top-1 accuracy on SSv2 without introducing additional computation or parameters, which outperforms most full fine-tuning methods, even though many of them have been pre-trained on the Kinetics dataset. And our ZeroI2V has a significant improvement compared to directly full fine-tuning ViT-L/16 pre-trained with CLIP (70.1 vs 48.7) with the same number of parameters and computation. Compared to other PETL methods, ZeroI2V outperforms ST-Adapter (Pan et al., 2022) on ViT-B/16 (70.1 vs 69.5) with lower GFLOPs (1688 vs 1955). Additionally, ZeroI2V significantly surpasses both EVL (Lin et al., 2022b) and AIM (Yang et al., 2023) (71.4 vs 66.7, 70.6) on ViT-L/14 with much lower GFLOPs (3892 vs 9641, 11508) and new parameters (0M vs 175M, 50M).

Table 4: **Results on Something-Something v2 validation set.** K400†/K600† indicates that the model is pre-trained on both IN21K (except for Uniformer (Li et al., 2022b) which uses IN1K) and K400/K600. The other notations are the same as Table 3.

| Methods | Pretrain | Views | GFLOPs | Extra GFLOPs | Param(M) | New Param(M) | Top-1 | Top-5 |
|--|----------|--------|--------|--------------|----------|--------------|-------------|-------------|
| <i>Methods with full fine-tuning</i> | | | | | | | | |
| TimeFormer-L (Bertasius et al., 2021) | IN21K | 64×3×1 | 7140 | - | 121 | - | 62.4 | - |
| ViViT-L (Arnab et al., 2021) | K400† | 16×3×4 | 11892 | - | 311 | - | 65.4 | 89.8 |
| MTV-B(†320) (Yan et al., 2022) | K400† | 32×3×4 | 11160 | - | 310 | - | 68.5 | 90.4 |
| VideoSwin-B (Liu et al., 2022c) | K400† | 32×3×1 | 963 | - | 89 | - | 69.6 | 92.7 |
| MViTv2-L(†312) (Li et al., 2022c) | K400† | 40×3×1 | 8484 | - | 213 | - | 73.3 | 94.1 |
| UniFormer-B (Li et al., 2022b) | K600† | 32×3×1 | 777 | - | 50 | - | 71.2 | 92.8 |
| ViT-L/14 (Dosovitskiy et al., 2021) | CLIP | 8×3×1 | 1946 | 0 | 86 | 0 | 48.7 | 77.5 |
| ILA ViT-L/14 (Tu et al., 2023) | CLIP | 8×3×4 | 10884 | 3100 | 529 | 225 | 67.8 | 90.5 |
| <i>Methods with PETL</i> | | | | | | | | |
| ST-Adapter ViT-B/16 (Pan et al., 2022) | CLIP | 32×3×1 | 1955 | 267 | 100 | 14 | 69.5 | 92.6 |
| EVL ViT-L/14 (Lin et al., 2022b) | CLIP | 32×3×1 | 9641 | 1858 | 479 | 175 | 66.7 | - |
| AIM ViT-L/14 (Yang et al., 2023) | CLIP | 32×3×1 | 11508 | 3725 | 354 | 50 | 70.6 | 92.7 |
| ZeroI2V ViT-B/16 | CLIP | 8×3×1 | 422 | 0 | 86 | 0 | 67.7 | 90.8 |
| ZeroI2V ViT-B/16 | CLIP | 16×3×1 | 844 | 0 | 86 | 0 | 69.4 | 91.7 |
| ZeroI2V ViT-B/16 | CLIP | 32×3×1 | 1688 | 0 | 86 | 0 | 70.1 | 92.4 |
| ZeroI2V ViT-L/14 | CLIP | 8×3×1 | 1946 | 0 | 304 | 0 | 70.1 | 91.8 |
| ZeroI2V ViT-L/14 | CLIP | 16×3×1 | 3892 | 0 | 304 | 0 | 71.4 | 93.0 |
| ZeroI2V ViT-L/14 | CLIP | 32×3×1 | 7783 | 0 | 304 | 0 | 72.2 | 93.0 |

Table 5: **Inference latency and throughput.** All results are obtained using a same V100-32G with PyTorch-builtin mixed precision, using a batch size of 1 to measure latency and the optimal possible batch size to measure throughput before running out of memory.

| Model | Views | GFLOPs | Latency (ms) | Throughput (V/s) | K400 Top-1 | SSv2 Top-1 |
|-------------------------------------|-------|--------|--------------|------------------|-------------|-------------|
| Uniformer-B (Li et al., 2022b) | 32×4 | 1036 | 245.38 | 4.24 | 82.9 | - |
| EVL ViT-B/16 (Lin et al., 2022b) | 8×3 | 454 | 53.87 | 24.04 | 82.9 | 61.0 |
| ViT-B/16 (Dosovitskiy et al., 2021) | 8×3 | 422 | 28.72 | 40.08 | 81.0 | 44.0 |
| ZeroI2V ViT-B/16 (Ours) | 8×3 | 422 | 28.89 | 40.08 | 83.0 | 67.7 |

Results on UCF101 and HMDB51 On two relatively small datasets, our method achieves top-1 accuracies of **98.6%** and **83.4%** on UCF101 and HMDB51, respectively. This demonstrates a clear performance advantage over both full-finetuning methods and PETL methods previously. More comparison with the state-of-the-art methods could be found in the Table 9 of Appendix B

Comparison of inference efficiency We compared the inference efficiency of our method with other methods on the same hardware device. As shown in Table 5, under comparable accuracy, the throughput of our method is 10 times that of Uniformer (Li et al., 2022b), Compared to the original ViT-B, our method introduces negligible additional latency during inference while achieving superior performance. In comparison with EVL (Lin et al., 2022b), it can also be seen that the impact of the additional computational module on the actual runtime latency (28.89 ms vs 53.87 ms) is greater than that reflected by GFLOPs (422 vs 454).

5 CONCLUSIONS

In this work, we have presented a new zero-cost approach for *parameter-efficient image-to-video transfer learning*, called ZeroI2V. By fully leveraging the powerful representational capabilities of pre-trained image models, our approach enables image transformers to perform video tasks without introducing extra cost during inferences. Our proposed STDHA achieves efficient spatial-temporal modeling at zero extra computation and parameters. In addition, through structural reparameterization and full adaptation strategies, we have successfully attempted to use a linear structure to achieve zero-cost image-to-video adaptation for the first time. ZeroI2V shows strong performance compared to previous full fine-tuning and PETL methods on four widely-used action recognition benchmarks while maintaining advantages in parameter and inference efficiency. Due to the simplicity and versatility of our method, we believe it can be easily extended to other video tasks and even multi-modal understanding tasks. We will further investigate this direction in future work.

Reproducibility To ensure all the results can be reproduced, we give the details of the model and training hyperparameters in our experiments (see Appendix A). And we will publish our source code after the review process.

REFERENCES

- Anurag Arnab, Mostafa Dehghani, Georg Heigold, Chen Sun, Mario Lucic, and Cordelia Schmid. Vivit: A video vision transformer. In *Int. Conf. Comput. Vis.*, pp. 6816–6826, 2021.
- Lei Jimmy Ba, Jamie Ryan Kiros, and Geoffrey E. Hinton. Layer normalization. *arXiv preprint arXiv:1607.06450*, 2016.
- Hangbo Bao, Li Dong, Songhao Piao, and Furu Wei. Beit: BERT pre-training of image transformers. In *Int. Conf. Learn. Represent.*, 2022.
- Gedas Bertasius, Heng Wang, and Lorenzo Torresani. Is space-time attention all you need for video understanding? In *Int. Conf. Mach. Learn.*, volume 139, pp. 813–824, 2021.
- Tom Brown, Benjamin Mann, Nick Ryder, Melanie Subbiah, Jared D Kaplan, Prafulla Dhariwal, Arvind Neelakantan, Pranav Shyam, Girish Sastry, Amanda Askell, et al. Language models are few-shot learners. In *Adv. Neural Inform. Process. Syst.*, volume 33, pp. 1877–1901, 2020.
- Adrian Bulat, Juan-Manuel Pérez-Rúa, Swathikiran Sudhakaran, Brais Martínez, and Georgios Tzimiropoulos. Space-time mixing attention for video transformer. In *Adv. Neural Inform. Process. Syst.*, pp. 19594–19607, 2021.
- Mathilde Caron, Hugo Touvron, Ishan Misra, Hervé Jégou, Julien Mairal, Piotr Bojanowski, and Armand Joulin. Emerging properties in self-supervised vision transformers. In *Int. Conf. Comput. Vis.*, pp. 9630–9640, 2021.
- João Carreira and Andrew Zisserman. Quo vadis, action recognition? A new model and the kinetics dataset. In *IEEE Conf. Comput. Vis. Pattern Recog.*, pp. 4724–4733, 2017.
- Shoufa Chen, Chongjian Ge, Zhan Tong, Jiangliu Wang, Yibing Song, Jue Wang, and Ping Luo. Adaptformer: Adapting vision transformers for scalable visual recognition. In *Adv. Neural Inform. Process. Syst.*, 2022.
- Mehdi Cherti, Romain Beaumont, Ross Wightman, Mitchell Wortsman, Gabriel Ilharco, Cade Gordon, Christoph Schuhmann, Ludwig Schmidt, and Jenia Jitsev. Reproducible scaling laws for contrastive language-image learning. *arXiv preprint arXiv:2212.07143*, 2022.
- Ekin Dogus Cubuk, Barret Zoph, Jonathon Shlens, and Quoc Le. Randaugment: Practical automated data augmentation with a reduced search space. In *Adv. Neural Inform. Process. Syst.*, 2020.
- Jacob Devlin, Ming-Wei Chang, Kenton Lee, and Kristina Toutanova. Bert: Pre-training of deep bidirectional transformers for language understanding. In *Proceedings of NAACL-HLT*, pp. 4171–4186, 2019.
- Ali Diba, Mohsen Fayyaz, Vivek Sharma, M Mahdi Arzani, Rahman Yousefzadeh, Juergen Gall, and Luc Van Gool. Spatio-temporal channel correlation networks for action classification. In *Eur. Conf. Comput. Vis.*, pp. 284–299, 2018.
- Alexey Dosovitskiy, Lucas Beyer, Alexander Kolesnikov, Dirk Weissenborn, Xiaohua Zhai, Thomas Unterthiner, Mostafa Dehghani, Matthias Minderer, Georg Heigold, Sylvain Gelly, Jakob Uszkoreit, and Neil Houlsby. An image is worth 16x16 words: Transformers for image recognition at scale. In *Int. Conf. Learn. Represent.*, 2021.
- Haoqi Fan, Bo Xiong, Karttikeya Mangalam, Yanghao Li, Zhicheng Yan, Jitendra Malik, and Christoph Feichtenhofer. Multiscale vision transformers. In *Int. Conf. Comput. Vis.*, pp. 6804–6815, 2021.
- Christoph Feichtenhofer. X3D: expanding architectures for efficient video recognition. In *IEEE Conf. Comput. Vis. Pattern Recog.*, pp. 200–210, 2020.

- Christoph Feichtenhofer, Haoqi Fan, Jitendra Malik, and Kaiming He. Slowfast networks for video recognition. In *Int. Conf. Comput. Vis.*, pp. 6201–6210, 2019.
- Raghav Goyal, Samira Ebrahimi Kahou, Vincent Michalski, Joanna Materzynska, Susanne Westphal, Heuna Kim, Valentin Haenel, Ingo Fründ, Peter Yianilos, Moritz Mueller-Freitag, Florian Hoppe, Christian Thurau, Ingo Bax, and Roland Memisevic. The "something something" video database for learning and evaluating visual common sense. In *Int. Conf. Comput. Vis.*, pp. 5843–5851. IEEE Computer Society, 2017.
- Kaiming He, Haoqi Fan, Yuxin Wu, Saining Xie, and Ross B. Girshick. Momentum contrast for unsupervised visual representation learning. In *IEEE Conf. Comput. Vis. Pattern Recog.*, pp. 9726–9735, 2020.
- Kaiming He, Xinlei Chen, Saining Xie, Yanghao Li, Piotr Dollár, and Ross B. Girshick. Masked autoencoders are scalable vision learners. In *IEEE Conf. Comput. Vis. Pattern Recog.*, pp. 15979–15988, 2022a.
- Xuehai He, Chunyuan Li, Pengchuan Zhang, Jianwei Yang, and Xin Eric Wang. Parameter-efficient model adaptation for vision transformers. *arXiv preprint arXiv:2203.16329*, 2022b.
- Neil Houlsby, Andrei Giurgiu, Stanislaw Jastrzebski, Bruna Morrone, Quentin de Laroussilhe, Andrea Gesmundo, Mona Attariyan, and Sylvain Gelly. Parameter-efficient transfer learning for NLP. In *Int. Conf. Mach. Learn.*, volume 97, pp. 2790–2799, 2019.
- Edward J. Hu, Yelong Shen, Phillip Wallis, Zeyuan Allen-Zhu, Yuanzhi Li, Shean Wang, Lu Wang, and Weizhu Chen. Lora: Low-rank adaptation of large language models. In *Int. Conf. Learn. Represent.*, 2022.
- Menglin Jia, Luming Tang, Bor-Chun Chen, Claire Cardie, Serge Belongie, Bharath Hariharan, and Ser-Nam Lim. Visual prompt tuning. In *Eur. Conf. Comput. Vis.*, pp. 709–727, 2022.
- Chen Ju, Tengda Han, Kunhao Zheng, Ya Zhang, and Weidi Xie. Prompting visual-language models for efficient video understanding. In *Eur. Conf. Comput. Vis.*, pp. 105–124. Springer, 2022.
- Hildegard Kuehne, Hueihan Jhuang, Estíbaliz Garrote, Tomaso Poggio, and Thomas Serre. Hmdb: a large video database for human motion recognition. In *Int. Conf. Comput. Vis.*, pp. 2556–2563. IEEE, 2011.
- Brian Lester, Rami Al-Rfou, and Noah Constant. The power of scale for parameter-efficient prompt tuning. In *Proceedings of the 2021 Conference on Empirical Methods in Natural Language Processing*, pp. 3045–3059, 2021.
- Junnan Li, Dongxu Li, Caiming Xiong, and Steven C. H. Hoi. BLIP: bootstrapping language-image pre-training for unified vision-language understanding and generation. In *Int. Conf. Mach. Learn.*, volume 162, pp. 12888–12900, 2022a.
- Kunchang Li, Yali Wang, Peng Gao, Guanglu Song, Yu Liu, Hongsheng Li, and Yu Qiao. Uniformer: Unified transformer for efficient spatial-temporal representation learning. In *Int. Conf. Learn. Represent.*, 2022b.
- Tianhao Li and Limin Wang. Learning spatiotemporal features via video and text pair discrimination. *arXiv preprint arXiv:2001.05691*, 2020.
- Xiang Lisa Li and Percy Liang. Prefix-tuning: Optimizing continuous prompts for generation. In *Proceedings of the 59th Annual Meeting of the Association for Computational Linguistics and the 11th International Joint Conference on Natural Language Processing (Volume 1: Long Papers)*, pp. 4582–4597, 2021.
- Yan Li, Bin Ji, Xintian Shi, Jianguo Zhang, Bin Kang, and Limin Wang. TEA: temporal excitation and aggregation for action recognition. In *IEEE Conf. Comput. Vis. Pattern Recog.*, pp. 906–915, 2020.

- Yanghao Li, Chao-Yuan Wu, Haoqi Fan, Karttikeya Mangalam, Bo Xiong, Jitendra Malik, and Christoph Feichtenhofer. Mvitv2: Improved multiscale vision transformers for classification and detection. In *IEEE Conf. Comput. Vis. Pattern Recog.*, pp. 4794–4804, 2022c.
- Dongze Lian, Daquan Zhou, Jiashi Feng, and Xinchao Wang. Scaling & shifting your features: A new baseline for efficient model tuning. In *Adv. Neural Inform. Process. Syst.*, 2022.
- Ji Lin, Chuang Gan, Kuan Wang, and Song Han. TSM: temporal shift module for efficient and scalable video understanding on edge devices. *IEEE Trans. Pattern Anal. Mach. Intell.*, 44(5): 2760–2774, 2022a.
- Ziyi Lin, Shijie Geng, Renrui Zhang, Peng Gao, Gerard de Melo, Xiaogang Wang, Jifeng Dai, Yu Qiao, and Hongsheng Li. Frozen CLIP models are efficient video learners. In *Eur. Conf. Comput. Vis.*, volume 13695, pp. 388–404, 2022b.
- Meng Liu, Zhengyang Wang, and Shuiwang Ji. Non-local graph neural networks. *IEEE Trans. Pattern Anal. Mach. Intell.*, 44(12):10270–10276, 2022a.
- Ze Liu, Yutong Lin, Yue Cao, Han Hu, Yixuan Wei, Zheng Zhang, Stephen Lin, and Baining Guo. Swin transformer: Hierarchical vision transformer using shifted windows. In *Int. Conf. Comput. Vis.*, pp. 9992–10002, 2021a.
- Ze Liu, Han Hu, Yutong Lin, Zhuliang Yao, Zhenda Xie, Yixuan Wei, Jia Ning, Yue Cao, Zheng Zhang, Li Dong, Furu Wei, and Baining Guo. Swin transformer V2: scaling up capacity and resolution. In *IEEE Conf. Comput. Vis. Pattern Recog.*, pp. 11999–12009, 2022b.
- Ze Liu, Jia Ning, Yue Cao, Yixuan Wei, Zheng Zhang, Stephen Lin, and Han Hu. Video swin transformer. In *IEEE Conf. Comput. Vis. Pattern Recog.*, pp. 3192–3201, 2022c.
- Zhaoyang Liu, Limin Wang, Wayne Wu, Chen Qian, and Tong Lu. TAM: temporal adaptive module for video recognition. In *Int. Conf. Comput. Vis.*, pp. 13688–13698, 2021b.
- Chengze Lu, Xiaojie Jin, Zhicheng Huang, Qibin Hou, Ming-Ming Cheng, and Jiashi Feng. CMAE-V: contrastive masked autoencoders for video action recognition. *arXiv preprint arXiv:2301.06018*, 2023.
- Paul Michel, Omer Levy, and Graham Neubig. Are sixteen heads really better than one? In *Adv. Neural Inform. Process. Syst.*, pp. 14014–14024, 2019.
- Bolin Ni, Houwen Peng, Minghao Chen, Songyang Zhang, Gaofeng Meng, Jianlong Fu, Shiming Xiang, and Haibin Ling. Expanding language-image pretrained models for general video recognition. In *Eur. Conf. Comput. Vis.*, volume 13664, pp. 1–18, 2022.
- Xing Nie, Bolin Ni, Jianlong Chang, Gaomeng Meng, Chunlei Huo, Zhaoxiang Zhang, Shiming Xiang, Qi Tian, and Chunhong Pan. Pro-tuning: Unified prompt tuning for vision tasks. *arXiv preprint arXiv:2207.14381*, 2022.
- Maxime Oquab, Timothée Darcet, Théo Moutakanni, Huy Vo, Marc Szafraniec, Vasil Khalidov, Pierre Fernandez, Daniel Haziza, Francisco Massa, Alaaeldin El-Nouby, Mahmoud Assran, Nicolas Ballas, Wojciech Galuba, Russell Howes, Po-Yao Huang, Shang-Wen Li, Ishan Misra, Michael G. Rabbat, Vasu Sharma, Gabriel Synnaeve, Hu Xu, Hervé Jégou, Julien Mairal, Patrick Labatut, Armand Joulin, and Piotr Bojanowski. DINOv2: Learning robust visual features without supervision. *arXiv preprint arXiv:2304.07193*, 2023.
- Junting Pan, Ziyi Lin, Xiatian Zhu, Jing Shao, and Hongsheng Li. St-adapter: Parameter-efficient image-to-video transfer learning. In *Adv. Neural Inform. Process. Syst.*, 2022.
- Jonas Pfeiffer, Andreas Rücklé, Clifton Poth, Aishwarya Kamath, Ivan Vulić, Sebastian Ruder, Kyunghyun Cho, and Iryna Gurevych. Adapterhub: A framework for adapting transformers. In *Proceedings of the 2020 Conference on Empirical Methods in Natural Language Processing: System Demonstrations*, pp. 46–54, 2020.

- Jonas Pfeiffer, Aishwarya Kamath, Andreas Rücklé, Kyunghyun Cho, and Iryna Gurevych. Adapterfusion: Non-destructive task composition for transfer learning. In *Proceedings of the 16th Conference of the European Chapter of the Association for Computational Linguistics: Main Volume*, pp. 487–503, 2021.
- Alec Radford, Karthik Narasimhan, Tim Salimans, Ilya Sutskever, et al. Improving language understanding by generative pre-training. *OpenAI blog*, 2018.
- Alec Radford, Jeffrey Wu, Rewon Child, David Luan, Dario Amodei, Ilya Sutskever, et al. Language models are unsupervised multitask learners. *OpenAI blog*, 1(8):9, 2019.
- Alec Radford, Jong Wook Kim, Chris Hallacy, Aditya Ramesh, Gabriel Goh, Sandhini Agarwal, Girish Sastry, Amanda Askell, Pamela Mishkin, Jack Clark, Gretchen Krueger, and Ilya Sutskever. Learning transferable visual models from natural language supervision. In *Int. Conf. Mach. Learn.*, volume 139, pp. 8748–8763, 2021.
- Ramprasaath R. Selvaraju, Michael Cogswell, Abhishek Das, Ramakrishna Vedantam, Devi Parikh, and Dhruv Batra. Grad-cam: Visual explanations from deep networks via gradient-based localization. *Int. J. Comput. Vis.*, 128(2):336–359, 2020.
- Khurram Soomro, Amir Roshan Zamir, and Mubarak Shah. Ucf101: A dataset of 101 human actions classes from videos in the wild. *arXiv preprint arXiv:1212.0402*, 2012.
- Zhan Tong, Yibing Song, Jue Wang, and Limin Wang. Videomae: Masked autoencoders are data-efficient learners for self-supervised video pre-training. In *Adv. Neural Inform. Process. Syst.*, 2022.
- Michael Tschannen, Basil Mustafa, and Neil Houlsby. Clippo: Image-and-language understanding from pixels only. *arXiv preprint arXiv:2212.08045*, 2022.
- Shuyuan Tu, Qi Dai, Zuxuan Wu, Zhi-Qi Cheng, Han Hu, and Yu-Gang Jiang. Implicit temporal modeling with learnable alignment for video recognition. In *Int. Conf. Comput. Vis.*, 2023.
- Limin Wang, Yuanjun Xiong, Zhe Wang, Yu Qiao, Dahua Lin, Xiaoou Tang, and Luc Van Gool. Temporal segment networks: Towards good practices for deep action recognition. In *Eur. Conf. Comput. Vis.*, volume 9912, pp. 20–36, 2016.
- Limin Wang, Zhan Tong, Bin Ji, and Gangshan Wu. TDN: temporal difference networks for efficient action recognition. In *IEEE Conf. Comput. Vis. Pattern Recog.*, pp. 1895–1904, 2021a.
- Limin Wang, Bingkun Huang, Zhiyu Zhao, Zhan Tong, Yinan He, Yi Wang, Yali Wang, and Yu Qiao. Videomae V2: scaling video masked autoencoders with dual masking. In *IEEE Conf. Comput. Vis. Pattern Recog.*, 2023.
- Mengmeng Wang, Jiazheng Xing, and Yong Liu. Actionclip: A new paradigm for video action recognition. *arXiv preprint arXiv:2109.08472*, 2021b.
- Rui Wang, Dongdong Chen, Zuxuan Wu, Yinpeng Chen, Xiyang Dai, Mengchen Liu, Yu-Gang Jiang, Luowei Zhou, and Lu Yuan. BEVT: BERT pretraining of video transformers. In *IEEE Conf. Comput. Vis. Pattern Recog.*, pp. 14713–14723, 2022.
- Wenhao Wu, Zhun Sun, and Wanli Ouyang. Revisiting classifier: Transferring vision-language models for video recognition. In *AAAI Conf. Artif. Intell.*, pp. 2847–2855, 2023.
- Wangmeng Xiang, Chao Li, Biao Wang, Xihan Wei, Xian-Sheng Hua, and Lei Zhang. Spatiotemporal self-attention modeling with temporal patch shift for action recognition. In *Eur. Conf. Comput. Vis.*, volume 13663, pp. 627–644, 2022.
- Saining Xie, Chen Sun, Jonathan Huang, Zhuowen Tu, and Kevin Murphy. Rethinking spatiotemporal feature learning: Speed-accuracy trade-offs in video classification. In *Eur. Conf. Comput. Vis.*, pp. 305–321, 2018.
- Shen Yan, Xuehan Xiong, Anurag Arnab, Zhichao Lu, Mi Zhang, Chen Sun, and Cordelia Schmid. Multiview transformers for video recognition. In *IEEE Conf. Comput. Vis. Pattern Recog.*, pp. 3323–3333, 2022.

- Taojiannan Yang, Yi Zhu, Yusheng Xie, Aston Zhang, Chen Chen, and Mu Li. Aim: Adapting image models for efficient video action recognition. In *Int. Conf. Learn. Represent.*, 2023.
- Elad Ben Zaken, Yoav Goldberg, and Shauli Ravfogel. Bitfit: Simple parameter-efficient fine-tuning for transformer-based masked language-models. In *Proceedings of the 60th Annual Meeting of the Association for Computational Linguistics (Volume 2: Short Papers)*, pp. 1–9, 2022.
- Xiaohua Zhai, Alexander Kolesnikov, Neil Houlsby, and Lucas Beyer. Scaling vision transformers. In *IEEE Conf. Comput. Vis. Pattern Recog.*, pp. 1204–1213, 2022.
- Guozhen Zhang, Yuhan Zhu, Haonan Wang, Youxin Chen, Gangshan Wu, and Limin Wang. Extracting motion and appearance via inter-frame attention for efficient video frame interpolation. In *IEEE Conf. Comput. Vis. Pattern Recog.*, 2023.
- Hao Zhang, Yanbin Hao, and Chong-Wah Ngo. Token shift transformer for video classification. In *ACM Int. Conf. Multimedia*, pp. 917–925, 2021.
- Yuanhan Zhang, Kaiyang Zhou, and Ziwei Liu. Neural prompt search. *arXiv preprint arXiv:2206.04673*, 2022.
- Zhun Zhong, Liang Zheng, Guoliang Kang, Shaozi Li, and Yi Yang. Random erasing data augmentation. In *AAAI Conf. Artif. Intell.*, pp. 13001–13008, 2020.
- Bolei Zhou, Alex Andonian, Aude Oliva, and Antonio Torralba. Temporal relational reasoning in videos. In *Eur. Conf. Comput. Vis.*, volume 11205, pp. 831–846, 2018.
- Mohammadreza Zolfaghari, Kamaljeet Singh, and Thomas Brox. Eco: Efficient convolutional network for online video understanding. In *Eur. Conf. Comput. Vis.*, pp. 695–712, 2018.

In this appendix, we provide more details of ZeroI2V from the following aspects:

- Implementation details of our method are in § A.
- Experimental results with other pre-trained weights and backbone architectures, as well as training cost analysis, can be found in § B.
- Visualization of our proposed Spatial-Temporal Dual-Headed Attention (STDHA) is in § C.
- Limitations and societal impact are in § D
- License of the datasets and pre-trained models are in § E

A IMPLEMENTATION DETAILS OF OUR METHOD

A.1 MODEL DETAILS

Table 6: **Model details.** We use a multiset to represent the time offsets of different heads (*e.g.*, "1 · 2" means that there are 2 heads with $\Delta t = 1$). When $\Delta t = 0$, it represents a spatial head. "Temporal RF" refers to temporal receptive field of a single STDHA. "Num. Adapters" refers to the number of linear adapters per ViT block.

(a) Model details for Kinetics400.

| Backbone | Frames | Δt of heads | Temporal RF | Num. Adapters |
|---------------------|--------|--|-------------|---------------|
| ViT-B ($h=12$) | 8 | $\{1 \cdot 1, -1 \cdot 1, 0 \cdot 10\}$ | 3 | 4 |
| | 16 | $\{1 \cdot 1, -1 \cdot 1, 2 \cdot 1, 0 \cdot 9\}$ | 4 | 4 |
| | 32 | $\{1 \cdot 1, -1 \cdot 1, 2 \cdot 1, -2 \cdot 1, 3 \cdot 1, 0 \cdot 7\}$ | 6 | 4 |
| ViT-L ($h=16$) | 8 | $\{1 \cdot 2, -1 \cdot 2, 0 \cdot 12\}$ | 3 | 4 |
| | 16 | $\{1 \cdot 2, -1 \cdot 2, 2 \cdot 1, 0 \cdot 11\}$ | 4 | 4 |
| | 32 | $\{1 \cdot 2, -1 \cdot 2, 2 \cdot 1, -2 \cdot 1, 3 \cdot 1, 0 \cdot 9\}$ | 6 | 4 |

(b) Model details for Something-Something v2.

| Backbone | Frames | Δt of heads | Temporal RF | Num. Adapters |
|----------------------------------|--------|--|-------------|---------------|
| ViT-B ($h=12$) | 8 | $\{1 \cdot 1, -1 \cdot 1, 0 \cdot 10\}$ | 3 | 6 |
| | 16 | $\{1 \cdot 1, -1 \cdot 1, 2 \cdot 1, -2 \cdot 1, 0 \cdot 8\}$ | 5 | 4 |
| | 32 | $\{1 \cdot 1, -1 \cdot 1, 2 \cdot 1, -2 \cdot 1, 3 \cdot 1, 0 \cdot 7\}$ | 6 | 4 |
| ViT-L ($h=16$) | 8 | $\{1 \cdot 2, -1 \cdot 2, 0 \cdot 12\}$ | 3 | 4 |
| | 16 | $\{1 \cdot 2, -1 \cdot 2, 2 \cdot 2, -2 \cdot 2, 0 \cdot 8\}$ | 5 | 4 |
| | 32 | $\{1 \cdot 2, -1 \cdot 2, 2 \cdot 1, -2 \cdot 1, 3 \cdot 1, 0 \cdot 9\}$ | 6 | 4 |
| Swin-B ($h = 4, 8, 16, 32$) | 32 | Stage 1: $\{1 \cdot 1, 0 \cdot 3\}$ | 2 | 4 |
| | | Stage 2: $\{1 \cdot 1, -1 \cdot 1, 0 \cdot 6\}$ | 3 | |
| | | Stage 3: $\{1 \cdot 1, -1 \cdot 1, 2 \cdot 1, -2 \cdot 1, 0 \cdot 12\}$ | 5 | |
| | | Stage 4: $\{1 \cdot 2, -1 \cdot 2, 2 \cdot 2, -2 \cdot 2, 0 \cdot 24\}$ | 5 | |

Our model details are shown in the Table 6a and Table 6b. Due to different requirements for spatial modeling and temporal modeling in different datasets, there are slight differences in the specific implementation settings.

Settings of STDHA For the settings of STDHA, we allocate 1/6 to 1/4 of the heads for temporal modeling based on the conclusions obtained from previous ablation experiments. For long inputs, we increase the absolute value of Δt to obtain a larger temporal receptive field. When using Swin-B as the backbone, due to its four stages and different numbers of heads in each stage, we simply allocate temporal heads to each stage at a ratio of 1/4. Since its input length is halved after patch embedding (from 32 frames to 16 frames), we set the value of Δt according to the best temporal receptive field of 16 frames, which is 5. Please note that we have not tried other configurations due to time constraints, so there may be better configurations.

Number of adapters Considering the balance between performance and training cost, we only assign different adapters for each weight for the minimum setting (ViT-B with 8-frame input) on the SSv2 dataset, which requires 6 adapters. For all other settings, we only use 4 adapters. And the bottleneck ratios of all adapters are set to 0.25.

A.2 TRAINING DETAILS

Table 7: **Training details of our method.**

| dataset | K400 | SSv2 |
|-------------------------------------|--|---|
| <i>Optimization settings</i> | | |
| optimizer | AdamW, learning rate=3e-4, weight decay=5e-2 | |
| batch size | 64 | |
| training epochs | 40 | 50 |
| <i>Sampling settings</i> | | |
| crop size | 224 | |
| frame sampling rate | 16 (for 8-frame input) 8 (for 16-frame input) 4 (for 32-frame input) | uniformly sample as TSN (Wang et al., 2016) |
| num. testing views | 3 temporal \times 1 spatial | 1 temporal \times 3 spatial |
| <i>Data augmentation settings</i> | | |
| RandAugment (Cubuk et al., 2020) | m=7, n=4 | |
| flip | 0.5 | |
| Random erasing (Zhong et al., 2020) | - | 0.25 |
| label smoothing | - | 0.1 |

As shown in the Table 7, our training strategy is similar to the previous methods (Pan et al., 2022; Yang et al., 2023). Considering that SSv2 requires stronger temporal modeling ability, we used a stronger data augmentation strategy following Liu et al. (2022c). In addition, for the full finetuning experiment using Swin-B as the backbone (Swin-B with STDHA), we use exactly the same training strategy as video swin transformer (Liu et al., 2022c).

Implementation details of adaptation strategies The training configurations used for all the adaptation strategies are summarized as follows:

- For the comparison experiment of full finetuning ViT with CLIP pretrained, we use 1/10 of the learning rate to avoid training collapse.
- For the comparison experiment of only tuning temporal head, we froze the parameters related to the spatial head (only training the part of the parameters related to the temporal head, in other words, we only trained $W_{\text{attn}}^{Q^t}, W_{\text{attn}}^{K^t}, W_{\text{attn}}^{V^t} \in \mathbb{R}^{d \times d^t}, W_{\text{attn}}^{O^t} \in \mathbb{R}^{d^t \times d}$, where d^t is the number of channels of the temporal head).

For any settings not explicitly mentioned, we assume they align with the training settings of the Linear Adapter.

B ADDITIONAL EXPERIMENTAL RESULTS

Effect of bottleneck ratio As shown in Table 8, a bottleneck ratio of 0.25 achieves a good trade-off between performance and the number of parameters. Therefore, we choose 0.25 as the bottleneck ratio for all subsequent experiments.

Experiments with ImageNet21K pre-trained weights In order to investigate the adaptability of our method to different pre-trained weights, we conducted experiments using the same model and training settings on ImageNet21K pre-trained weights. The results are shown in Table 10. It can be seen that our method is still very effective under ImageNet21K weights and can surpass previous full

Table 8: **Effect of bottleneck ratio of linear adapters.**

| Ratio | Tunable Param(M) | Top-1 |
|--------|------------------|-------------|
| 0.0625 | 3 | 64.2 |
| 0.125 | 7 | 65.0 |
| 0.25 | 14 | 66.0 |
| 0.5 | 28 | 65.8 |

Table 9: **Comparing the state-of-the-art video recognition methods on UCF101 and HMDB51.** We following ST-Adapter [1] test our method and report the 3-split mean Top-1 accuracy for both datasets.

| Method | Pretrain | UCF101 | HMDB51 |
|--|---------------------|-------------|-------------|
| STC (Diba et al., 2018) | K400 | 95.8 | 72.6 |
| ECO (Zolfaghari et al., 2018) | K400 | 93.6 | 68.4 |
| I3D (Carreira & Zisserman, 2017) | ImageNet+K400 | 95.6 | 74.8 |
| S3D (Xie et al., 2018) | ImageNet+K400 | 96.8 | 75.9 |
| SlowOnly-8x8-R101 (Feichtenhofer et al., 2019) | Kinetics+OmniSource | 97.3 | 79.0 |
| VideoPrompt (Ju et al., 2022) | CLIP | 93.6 | 66.4 |
| ST-Adapter ViT-B/16 (Pan et al., 2022) | CLIP+K400 | 96.4 | 77.7 |
| ST-Adapter ViT-L/14 (Pan et al., 2022) | CLIP+K400 | 98.1 | 81.7 |
| ZeroI2V ViT-B/16 (Ours) | CLIP | 95.6 | 73.7 |
| ZeroI2V ViT-B/16 (Ours) | CLIP+K400 | 97.7 | 78.5 |
| ZeroI2V ViT-L/14 (Ours) | CLIP | 97.8 | 79.9 |
| ZeroI2V ViT-L/14 (Ours) | CLIP+K400 | 98.6 | 83.4 |

Table 10: **Results on K400 and SSv2 validation set with ImageNet21K pretrained.** Views = #frames \times #spatial crops \times #temporal clips. ‘‘GFLOPs’’ means 10^9 FLOPs, ‘‘M’’ means 10^6 . ‘‘Extra GLOPs’’ refers to the extra computation added to the original ViT under the same number of views. ‘‘New Params’’ refers to additional parameters during inference besides the parameters of the original ViT backbone and linear classifier. Views for all methods are $8 \times 1 \times 3$ for K400 and $8 \times 3 \times 1$ for SSv2

| Methods | Pretrain | GFLOPs | Extra GFLOPs | Param(M) | New Param(M) | K400 Top-1 | SSv2 Top-1 |
|--|----------|--------|--------------|----------|--------------|-------------|-------------|
| <i>Methods with full fine-tuning</i> | | | | | | | |
| TimeSformer (Bertasius et al., 2021) | IN21K | 590 | - | 121 | - | 78.0 | 59.5 |
| X-ViT (Bulat et al., 2021) | IN21K | 425 | - | 92 | - | 78.5 | 64.4 |
| <i>Methods with PETL & CLIP ViT-B/16</i> | | | | | | | |
| EVL (Lin et al., 2022b) | IN21K | 454 | 32 | 115 | 29 | 75.4 | - |
| ST-Adapter (Pan et al., 2022) | IN21K | 455 | 33 | 93 | 7 | 76.6 | 62.8 |
| AIM (Yang et al., 2023) | IN21K | 624 | 202 | 100 | 14 | 78.8 | 62.0 |
| ZeroI2V | IN21K | 422 | 0 | 86 | 0 | 78.6 | 65.3 |

fine-tuning methods. Compared to other PETL methods, our method shows stronger robustness. As shown in Figure 1, when using ImageNet21K pre-trained weights, the advantage of our method over other PETL methods is even greater than when using CLIP pre-trained weights. For example, when using CLIP weights, our method slightly surpasses ST-Adapter (Pan et al., 2022) (67.7 vs 67.1), while when using ImageNet21K weights, we have a clear advantage (65.3 vs 62.8).

Table 11: **Results on SSv2 validation set with Swin-B backbone.** K400 \dagger indicates that the model is pre-trained on both IN21K and K400. The other notations are the same as Table 10

| Methods | Pretrain | Views | GFLOPs | Param(M) | Tunable Param(M) | Top-1 | Top-5 |
|---------------------------------|----------------|------------------------|--------|----------|------------------|-------------|-------------|
| VideoSwin-B (Liu et al., 2022c) | K400 \dagger | $32 \times 3 \times 1$ | 963 | 89 | 89 | 69.6 | 92.7 |
| PST-B (Xiang et al., 2022) | IN21K | $32 \times 3 \times 1$ | 741 | 89 | 89 | 67.4 | 90.9 |
| SIFAR-B (Xiang et al., 2022) | IN21K | $32 \times 3 \times 1$ | 789 | 87 | 87 | 62.6 | 88.5 |
| Swin-B w/ STDHA | IN21K | $32 \times 3 \times 1$ | 741 | 89 | 89 | 70.0 | 92.1 |
| ZeroI2V Swin-B | IN21K | $32 \times 3 \times 1$ | 741 | 89 | 14 | 67.8 | 91.4 |

Experiments with other backbone In order to verify the universality of our method, we conducted experiments using the Swin Transformer (Liu et al., 2021a) in Table 11, which has a hierarchical structure and local window attention. As shown in Table 1, although our method was not specifically

designed and adjusted for it, it can still achieve performance comparable or even better than other full fine-tuning methods. To our surprise, when we used a full fine-tuning strategy to train Swin-B using STDHA, we achieved a top-1 accuracy of **70%**, which even surpassed VideoSwin-B (Liu et al., 2022c) pre-trained on the K400 dataset. From this, we can see that our designed STHDA is not only versatile but also has powerful temporal modeling capabilities. In addition, for backbones like Swin Transformer that have more inductive bias and have not been trained on large-scale image-text datasets, full fine-tuning may be able to better utilize the temporal modeling capabilities of STDHA.

Comparison of training cost We compared the training cost of our method with previous methods in Table 12. It can be seen that compared to previous full fine-tuning methods such as Uniformer (Li et al., 2022b) and ActionCLIP (Wang et al., 2021b), our method significantly reduces training cost. However, due to the dense insertion of linear adapters during training, our training cost is slightly higher than that of previous PETL methods such as EVL (Lin et al., 2022b). However, we believe that it is worthwhile and acceptable to exchange some training cost for a reduction in inference cost. We will also try to further reduce training cost by improving training strategies and adaptation strategies in the future.

Table 12: **Comparison of training cost.** Our results are obtained using a same V100-32G with PyTorch-builtin mixed precision, following EVL (Lin et al., 2022b).

| Model (Frames) | Pretrain | Frames | Training GPU Hours | Tunable Param (M) | K400 Top-1 |
|--|----------|--------|--------------------|-------------------|-------------|
| Uniformer-B (Li et al., 2022b) | IN1K | 32 | 5000 × V100 | 50 | 82.9 |
| ActionCLIP ViT-B/16 (Wang et al., 2021b) | CLIP | 16 | 480 × RTX3090 | 142 | 82.6 |
| EVL ViT-B/16(Lin et al., 2022b) | CLIP | 8 | 60 × V100 | 29 | 82.9 |
| Zero12V ViT-B/16 (Ours) | CLIP | 8 | 85 × V100 | 14 | 83.0 |

C VISUALIZATION

The motivation behind the design of STDHA was to enable simultaneous spatial and temporal modeling in an independent way before information fusion (ie. decoupling spatial and temporal modeling). In order to more intuitively demonstrate the temporal modeling capabilities of our proposed STDHA, we visualized the attention map of the last layer of the network. As shown in Figure 3, note that we visualize the attention map of the last transformer layer in our figure. Due to the temporal receptive field increases with the network depth, both the spatial head and the temporal head of this last layer have a global temporal receptive field about the input frames. But we can still observe that the spatial heads pay more attention to the information of the current frame while the temporal head pays more attention to the information of other frames.

D LIMITATIONS AND SOCIETAL IMPACT

Limitations Our method has the following two main limitations:

- Although our method is very efficient during inference, the densely inserted linear adapters still need to participate in gradient calculation during training, which brings a non-negligible training cost. This makes our method still have a certain disadvantage in training cost compared to methods that use CLIP as an independent feature extractor (such as EVL (Lin et al., 2022b)). In the future, we need to consider more efficient training strategies and improve the structure of linear adapters to address this issue.
- Although STDHA has demonstrated powerful temporal modeling capabilities, it still requires consideration of the original number of heads in ViT and manual design of a head relocation strategy. Despite the ablation experiment results showing that our method’s performance is relatively stable across different head relocation strategies, achieving better results still necessitates some manual design. Obtaining optimal head relocation strategies through manual design is obviously challenging. In future work, we aim to investigate methods for automatically designing head relocation strategies.



Figure 3: Visualization of attention maps of spatial heads, temporal heads and STDHA at the last layer generated by Grad-CAM (Selvaraju et al., 2020) on SSV2 validation set.

Societal impact Our ZeroI2V method can apply existing image pre-trained transformers as powerful backbone networks for video tasks such as video classification, spatiotemporal action detection, and video segmentation. Although we do not provide direct applications, it still has the potential to be applied to many scenarios related to video tasks. On the positive side, a powerful video understanding backbone network can improve the performance of downstream tasks and thus enhance efficiency in various scenarios, such as in the fields of smart healthcare and intelligent transportation where video understanding is required. On the other hand, if applied improperly, advanced video networks may also have negative impacts, such as being used in terrorist military activities. Researchers need to carefully consider the potential risks and impacts when applying it to real-world scenarios.

E LICENSE OF DATASETS AND PRE-TRAINED MODELS

All the datasets we used are commonly used datasets for academic purpose. The license of the Kinetics-400¹ is CC BY-NC 4.0². The license of the Something-Something V2³ is custom. We used the publicly available CLIP pre-trained weights provided by OpenAI⁴ and the Swin Transformer pre-trained weights provided by Microsoft⁵, both of which use the MIT License.

¹<https://www.deepmind.com/open-source/kinetics>

²<https://creativecommons.org/licenses/by/4.0>

³<https://developer.qualcomm.com/software/ai-datasets/something-something>

⁴<https://github.com/openai/CLIP>

⁵<https://github.com/microsoft/Swin-Transformer>